Tmem45b is essential for inflammation and tissue injury-induced persistent mechanical hyperalgesia

Tadashi Tanioku
Wakayama Medical University School of Medicine
Masayoshi Nishibata
Wakayama Medical University School of Medicine
Yasuyuki Tokinaga
Wakayama Medical University School of Medicine
Kohtarou Konno
Hokkaido University
Masahiko Watanabe
Graduate School of Medicine, Hokkaido University
Hiroaki Hemmi
Okayama University of Science
Yuri Ohta
Wakayama Medical University School of Medicine
Tsuneyasu Kaisho
Wakayama Medical University School of Medicine
Tomoyuki Kawamata (kawamata@wakayama-med.ac.jp)
Wakayama Medical University School of Medicine https://orcid.org/0000-0003-1535-6715

Article

Keywords: Tmem45b, peripheral nervous system, mechanical hyperalgesia

Posted Date: September 1st, 2021

DOI: https://doi.org/10.21203/rs.3.rs-829215/v1

Title: **Tmem45b is essential for inflammation and tissue injury-induced persistent mechanical hyperalgesia**

Tadashi Tanioku[1], Masayoshi Nishibata[1], Yasuyuki Tokinaga[1], Kohtaro Konno[2], Masahiko Watanabe[2], Hiroaki Hemmi[3], Yuri Fukuda-Ohta[3], Tsuneyasu Kaisho[3], Tomoyuki Kawamata[1*]

1. Department of Anesthesiology, Wakayama Medical University School of Medicine, Wakayama, Japan
2. Department of Anatomy, Hokkaido University Graduate School of Medicine, Hokkaido, Japan
3. Department of Immunology, Institute of Advanced Medicine, Wakayama Medical University School of Medicine, Wakayama, Japan

*Corresponding author: Tomoyuki Kawamata (kawamata@wakayama-med.ac.jp)

Acknowledgements

We thank T. Ozasa at Department of Immunology, Institute of Advanced Medicine, Wakayama Medical University School of Medicine for generating KO mice. This study was supported by grants from JSPS KAKENHI Grant Numbers JP17H04322 (to T.Kaw.) and JP18K16460 (to T.T).

Author contributions

T.T. performed all experiments and analyzed data. Y.T. performed immunoblotting. M.N. and K.K. performed FISH and immunohistochemistry. M.W. generated an anti-Tmem45b antibody. T.Kai., H.H., and Y.F.-O. generated Tmem45b gene-deficient mice. T.Kaw. designed the experiments and wrote the manuscript. M.W., T.Kai. and H.H. reviewed the manuscript.

Competing interests

The authors declare no competing financial interests.

Abstract

Persistent mechanical hyperalgesia, associated with peripheral inflammation and tissue injury, impairs patient's quality of life and daily activity. However, its molecular mechanism and treatment are yet to be deciphered. Herein, we report that Tmeme45b is expressed in a subset of unmyelinated primary sensory neurons and plays an essential role in inflammation and tissue injury-induced mechanical hyperalgesia. Our findings provide new insights into the mechanisms and the treatment of mechanical hyperalgesia.

Main

Pain functions as a warning system to alert us to real or impending injury and trigger appropriate protective responses. In addition, pain is not just a passive consequence of the transfer of peripheral input to the brain but also an active process. Inflammation, tissue injury, and nerve injury can induce a decrease in the pain threshold and an increase in the pain intensity, so-called hyperalgesia[1]. Persistent hyperalgesia causes distress to humans beyond the warning signals, interfering with physical and mental activities. Therefore, persistent hyperalgesia is an important clinical problem to be solved. Hyperalgesia can be divided into two types according to the modality of stimuli: thermal hyperalgesia and mechanical hyperalgesia. Recent advances in neuroscience research have revealed molecules such as TRP channels responsible for thermal hyperalgesia[2]. On the other hand, mechanisms responsible for mechanical hyperalgesia in mammals remain poorly understood[3]. Herein, we discuss a molecule that is crucial for mechanical hyperalgesia observed in inflammation and tissue injury in mice.

Nociceptive stimuli are sensed and transmitted by small myelinated sensory neurons and unmyelinated sensory neurons. Unmyelinated sensory neurons can be divided into two classes by isolectin B4 (IB4)-binding[4,5]: IB4-not binding ($IB4^-$) neurons, which are peptidergic and mainly express TRPV1 or CGRP and IB4-binding ($IB4^+$) neurons, which are non-peptidergic[6,7]. Recent ablation studies have demonstrated that TRPV1- or CGRP-positive neurons are involved in heat pain and heat hyperalgesia but not in mechanical

pain[8,9]. However, the kind of pain IB4$^+$ neurons are involved in remains unknown. To examine the role of IB4$^+$ neurons in pain transmission, we selectively ablated IB4$^+$ neurons using IB4-saporin[10-11]. Intrasciatic nerve injection of IB4-saporin eliminated IB4$^+$ afferents but not CGRP-positive afferents (Fig. 1a, b), while injection of saporin alone did not (data not shown). Ablation of IB4$^+$ neurons had no effect on the withdrawal latency to noxious heat stimuli and the withdrawal threshold to von Frey filaments (Fig. 1c), confirming previous findings[11]. Next, we examined the role of IB4$^+$ neurons in three pain models with different neural mechanisms including a complete Freund's adjuvant (CFA)-induced inflammatory pain model, a skin incision-induced tissue injury pain model, and a peripheral nerve injury-induced neuropathic pain model. CFA injection and skin incision to the hindpaw induced a decrease in the withdrawal threshold to mechanical stimuli of von Frey filaments (mechanical hyperalgesia) and a decrease in the withdrawal latency to noxious heat stimuli (thermal hyperalgesia) in mice that received saproin (Fig. 1d, e). On the other hand, mice that received IB4-saporin showed thermal hyperalgesia but not mechanical hyperalgesia (Fig. 1d, e). The neuropathic pain model that we used shows mechanical hyperalgesia but not thermal hyperalgesia[12]. Both mice that received saporin and mice that received IB4-saporin also showed mechanical hyperalgesia but not thermal hyperalgesia (Fig. 1f), indicating that IB4$^+$ neurons are not involved in mechanical hyperalgesia in a neuropathic pain model. Taken together, the results show that IB4$^+$ neurons are selectively involved in inflammation and tissue injury-induced mechanical hyperalgesia, leading to the idea that molecules responsible for inflammation and tissue injury-induced mechanical hyperalgesia could be expressed in IB4$^+$ neurons.

To explore molecules responsible for inflammation and tissue injury-induced mechanical hyperalgesia, we compared gene expression profiles of dorsal root ganglia (DRGs) from mice that received either IB4-saporin or saporin using a cDNA array. Genes with an important difference in expression (>1.5-fold change) were selected, and 43 were identified as being predominantly expressed in IB4$^+$ neurons (Fig. 2a). Since Mishra et al.[13] reported 153 genes selectively expressed in somatosensory neurons, we focused on 12 genes that overlapped between our 43 identified genes and the 153 somatosensory-specific genes (Fig. 2b). Among the

12 genes, we decided to analyze *Tmem45b*, for which the function in the nervous system has not yet been reported.

Real-time quantitative PCR analysis revealed that *Tmem45b* was mainly expressed in DRGs, aorta, bladder, and digestive tracts (Fig. 2c). *Tmem45b* was rarely expressed in the spinal cord and supra-spinal regions. As expected, double staining by *in situ* hybridization and immunohistochemistry revealed that most of the $IB4^+$ neurons (91.8% ± 1.8%, n=4) were positive for *Tmem45b* mRNA in DRGs (Fig. 2d). Next, we examined Tmem45b expression using a specific antibody, validated by negative labeling in *Tmem45b*-knockout DRGs and co-labeling for *Tmem45b* mRNA in wild-type DRGs (Extended Data Fig. 1). Immunohistochemical analysis showed that the percentage of Tmem45b-positive neurons among the total DRG neurons was 38.1% ± 1.5% and that Tmem45b was selectively expressed in small-sized DRG neurons with an area <600 μm^2 and rarely expressed in medium to large-sized DRG neurons (Fig. 2e, f). Double staining with several neuronal makers showed that Tmem45b was expressed in most $IB4^+$ neurons (93.5 ± 2.4%), some TRPV1-positive neurons (19.1 ± 1.1%), and some CGRP-positive neurons (7.1 ± 1.3%), but was rarely expressed in NF200-positive neurons (0.1 ± 0.1%), which are considered to be myelinated sensory neurons (Fig. 2g and Supplementary Table 3). Next, we examined the central and peripheral projections of Tmem45-positive afferents. In the spinal cord, Tmem45b-positive central afferents mainly terminated in the dorsal part of lamina II inner, which comprises $IB4^+$ afferents (Fig. 2h and see Methods). A retrograde tracing experiment using Fast blue showed that 28.1% of DRG neurons innervating glabrous skin in the hindpaw and 35.9% of DRG neurons innervating the tibialis anterior muscle were Tmem45b-positive, whereas the percentage of Tmem45b-positive DRG innervating visceral organs (e.g., distal colon and bladder) was considerably low (Extended Data Fig. 2).

To clarify the role of Tmem45b in pain perception, we studied *Tmem45b* knockout mice (KO mice) (Fig. 3a and Extended Data Fig. 3). The KO mice were viable and did not show any overt motor defects or reflex

impairments (data not shown). The KO mice showed withdrawal latency to noxious heat stimuli and withdrawal threshold to von Frey filaments that were comparable to those of WT mice (Fig. 3b). We examined the contribution of Tmem45b to mechanical hyperalgesia in an inflammatory pain model using KO mice. CFA injection to the hindpaw resulted in long-lasting mechanical and thermal hyperalgesia in WT mice, whereas KO mice showed thermal hyperalgesia but not mechanical hyperalgesia throughout the observation period (Fig. 3c). In addition, CFA injection-induced paw edema was comparable in WT and KO mice, suggesting that Tmem45b is not involved in the development of local inflammation (Extended Data Fig. 4). To exclude the possibility of secondarily developmental influence by gene knockout, we conducted a knockdown experiment using siRNA. We confirmed that our siRNA against *Tmem45b* reduced *Tmem45b* mRNA in Lewis lung carcinoma cells to ~20% compared with scrambled siRNA (Extended Data Fig. 5). First, siRNA against *Tmem45b* was intrathecally administered before CFA injection (pre-treatment). Intrathecal injection of siRNA against *Tmem45b* or scrambled siRNA once a day for 3 consecutive days did not change withdrawal latency to noxious heat stimuli and withdrawal threshold to von Frey filaments compared with those before intrathecal administration (Fig. 3d upper panel). Twenty-four hours after the 3rd siRNA administration, CFA was injected into the hindpaw. The mice that received siRNA against *Tmem45b* developed thermal hyperalgesia, but mechanical hyperalgesia was significantly prevented compared to that that received scrambled siRNA (Fig. 3d, upper). In addition, effects of siRNA against *Tmem45b* on established hyperalgesia after CFA injection (post-treatment) were examined (Fig. 3d, lower). Since CFA-induced hyperalgesia was maintained from 4 to

168 hr after CFA injection, siRNA was administered at 24, 48, and 72 hr after CFA injection. Intrathecal injection of siRNA against *Tmem45b* partially improved mechanical hyperalgesia compared to injection of scrambled siRNA. In both pre- and post-treatment with siRNA, siRNA against *Tmem45b* significantly decreased *Tmem45b* mRNA levels in DRGs compared with scrambled siRNA (Fig. 3e). These results suggest that inhibition of CFA-induced mechanical hyperalgesia observed in KO mice is not due to secondarily developmental change of the nervous system induced by downregulation of Tmem45b but is due to direct involvement of Tmem45b in the development and maintenance of CFA-induced mechanical hyperalgesia.

Finally, we examined the involvement of Tmem45b in hyperalgesia observed in different pain models including the skin incision-induced tissue injury pain model and the peripheral nerve injury-induced neuropathic pain model. Although WT mice showed skin incision-induced thermal and mechanical hyperalgesia, KO mice showed thermal hyperalgesia but not mechanical hyperalgesia, similar to the results obtained in the CFA-induced inflammation pain model (Fig. 3f). In the neuropathic pain model, nerve injury-induced hyperalgesia was comparable in WT mice and KO mice (Fig. 3g), indicating that Tmem45b is not involved in nerve injury-induced hyperalgesia.

It has been reported that Tmem45b is involved in the development of several types of cancer[14-17]. In this study, we demonstrated for the first time that Tmem45b does not play a role in sensing noxious mechanical stimuli under normal conditions but is essential for inflammation and tissue injury-induced mechanical hyperalgesia. The molecular mechanisms controlled by Tmem45b in inflammation or tissue injury-induced

mechanical hyperalgesia remain to be elucidated. Although an *in silico* study has suggested that Tmem45b is a7-transmembrane protein[18], Tmem45b does not have any typical amino acid sequences of G protein-coupled receptors (GPCRs) such as the CWxP motif in TM6, NPxxY motif in TM7, or D/ERY motif in TM3[19]. This suggests that Tmem45b does not belong to the family of GPCRs. Further studies will be necessary to clarify the molecular function of Tmem45b and the mechanisms of Tmem45b-induced mechanical hyperalgesia. A therapeutic approach targeting Tmem45b is attractive for two reasons. One reason is that it does not affect physiological pain sensitivity, and it can therefore relieve pathological pain while retaining pain as a warning signal. The other reason is that Tmem45b is mainly expressed in peripheral neurons and is rarely expressed in central neurons. Therefore, such a therapeutic approach may avoid the possible side effects associated with the central nervous system including addiction, which is known to lead to serious health concerns in opioid therapy, the so-called "opioid crisis"[20].

References

1. Treede, R.D,. et al. Peripheral and central mechanisms of cutaneous yperalgesia. *Prog Neurobiol* **38**, 397-421, (1992)
2. Vriens, J., Nilius ,B. & Voets, T. Peripheral thermosensation in mammals. *Nat. Rev. Neurosci.* **15**, 573-589 (2014)
3. Hill, R.Z. & Bautista, D.M. Getting in touch with mechanical pain mechanisms. *Trends in Neurosci*. **43**, 311-325 (2020)
4. Silverman, J.D. & Kruger, L. Selective neuronal glycoconjugate expression in sensory and autonomic ganglia: relation of lectin reactivity to peptide and enzyme markers. *J Neurocytol*. **19**, 789-801 (2020)
5. Nagy, J.I. & Hunt, S.P. Fluoride-resistant acid phosphatase-containing neurones in dorsal root ganglia are separate from those containing substance P or somatostatin. *Neuroscience* **7**, 89-97 (1982)
6. Zwick, M., et al. Glial cell line-derived neurotrophic factor is a survival factor for isolectin B4-positive, but not vanilloid receptor 1-positive, neurons in the mouse. *J Neurosci*. **22**, 4057-4065 (2002)
7. Woodbury, C.J., et al. Nociceptors lacking TRPV1 and TRPV2 have normal heat responses. *J Neurosci*. **24**, 6410-6415 (2004)
8. McCoy, E.S., et al. Peptidergic CGRPα primary sensory neurons encode heat and itch and tonically suppress sensitivity to cold. *Neuron* **8**, 138-151 (2013)
9. Cavanaugh, D.J., et al. Distinct subsets of unmyelinated primary sensory fibers mediate behavioral responses to noxious thermal and mechanical stimuli. *Proc. Natl. Acand. Sci*. **106**, 9075-9080 (2009)
10. Ono, K., et al. TRPV1 expression level in isolectin B_4-positive neurons contributes to mouse strain difference in cutaneous thermal nociceptive sensitivity. *J. Neurophysiol.* **113**, 3345-3355 (2015)
11. Pinto, L.G., et al. Non-peptidergic nociceptive neurons are essential for mechanical inflammatory hypersensitivity in mice. *Mol. Neurobiol.* **56**, 5715-5728 (2019)

12. Holmes, F.E., et al. Transgenic overexpression of galanin in the dorsal root ganglion modulates pain-related behaviors. *Proc. Natl. Acand. Sci*. **100,** 6180-6185 (2013)

13. Mishra, S.K., Holzman, S. & Hoon, M.A. A nociceptive signaling role for neuromedin B. *J. Neurosci*. **32**, 8686-8695 (2012)

14. Shen, K., et al. Knockdown of TMEM45B inhibits cell proliferation and invasion in gastric cancer. *Biomed. Pharmacother*. **104**, 576-81 (2018)

15. Li, Y., et al. Silencing transmembrane protein 45B (TNEM45B) inhibits proliferation, invasion, and tumorigenesis in osteosarcoma cells. *Oncol. Res*. **25**, 1021-1026 (2017)

16. Hu, R., et al. TMEM45B, up-regulated in human lung cancer, enhances tumorigenicity of lung cancer cells. *Tumor Biol*. **37**, 12181-12191 (2016)

17. Zhao, L.C., et al. TMEM45B promotes proliferation, invasion and migration and inhibits apoptosis in pancreatic cancer cells. *Mol. Biosyst.* **12**, 1860-1870 (2016)

18. Wrzesinski, T., et al. Expression of pre-selected TMEMs with predicted ER localization as potential classifiers of ccRCC tumors. *BMC. Cancer* **15**, 518 (2015)

19. Filipek, S. Molecular switches in GPCRs. *Curr. Opin. Struct. Biol.* **55**, 114-120 (2019)

20. Volkow, N.D. & Collins, F.S.C. The role of science in addressing the opioid crisis. *N Engl J Med*. **377**, 391-394 (2017)

Methods

Animals

Approval was obtained from the Wakayama Medical University Animal Care and Use Committee for all the procedures of this study that were in accordance with the ethical guidelines of the National Institutes of Health and of the International Association for the study of Pain. Adult male C57BL/6N mice (20–25 g, Japan SLC, Japan) and Tmem45b-deficient mice of C57BL/6N strain (20–25 g) were used for experiments. The mice were housed in a temperature-controlled (21°C ± 1°C) room under a 12 h light/dark cycle and were given food and water ad libitum. Behavioral tests were conducted at 7–12 weeks-of-age.

Deletion of IB4 positive afferents in sciatic nerve

Using 3% sevoflurane, B6 mice were anesthetized. Then, to expose the sciatic nerve, a small incision was made on the skin of the leg proximal to the knee and the skin and underlying muscle opened by blunt dissection. A needle of 29.5 gauge was attached to a 10 μl syringe (Hamilton, Reno, NV, USA), and 1 μl of IB4-saporin (1 μg/μl saline; Advanced Targeting Systems, San Diego, CA, USA) or saporin (1 μg/μl saline) were injected as control into the left sciatic nerve. The muscle tissue was closed back over the nerves and then skin was sutured shut using 6-0 nylon sutures. Any animals displaying motor impairment during recovery were immediately euthanized. Animals without any motor impairment were used for the experiments 7–10 days after intrasciatic injection. After the behavioral experiment, the deletion of IB4 positive afferents was checked

by IB4 binding in dorsal horn of the L4–5 spinal cord.

Generation of *Tmem45b* KO mice

We generated *Tmem45b* knockout mice by using CRISPR/Cas9 technology. The guide RNAs (gRNAs) for targeting *Tmem45b* were designed by Invitrogen™ GeneArt™ CRISPR Search and Design Tool (Thermo Fisher Scientific, Waltham, MA, USA) and synthesized using GeneArt™ Precision gRNA Synthesis Kit (Thermo Fisher Scientific) (Supplementary Table 1). Cas9 endonuclease mRNA was generated via *in vitro* transcription using MEGAshortscript T7 (Thermo Fisher Scientific) and purified using MEGAclear kit (Thermo Fisher Scientific). One cell-stage fertilized embryos from B6C3F1 females mated with C57BL/6N males were injected with the gRNAs and Cas9 mRNA and transferred to the oviducts of pseudopregnant foster mice. Founders bearing deletion of *Tmem45b* were identified by PCR with the primers, Tmem45b-1 and Tmem45b-2, which should yield a 4282- and 1181-bp product from the wild-type and mutated alleles (Supplementary Table 2). Mutant mice were backcrossed to C57BL/6N mice.

Knockdown of *Tmem45b*

Preparation of siRNA against Tmem45b and scrambled siRNA

siRNA against mice *Tmem45b* were purchased from Sigma Aldrich (St. Louis, MO, USA). Sense and antisense siRNA sequences were: 5′-CUUAUGUGCUCCUAGGGCU-3′ and 5′-AGCCCUAGGACACAUAAG-3′. A

scrambled control siRNA without significant homology to any known mouse gene sequence was obtained from Sigma Aldrich. For *in vivo* siRNA transfer, the hemagglutinating virus of the Japan (HVJ) envelope vector system (HVJ Envelope Vector Kit GenomONE-Neo; Ishihara Sangyo Kabushikigaisya, Ltd., Osaka, Japan) was used. siRNA was incorporated into the HVJ-envelope vector as per the manufacturer's instructions, as reported previously[21]. In brief, the mixture was centrifuged (10,000 g, 10 min, 4°C) and the pellet was suspended in 10 µl of buffer solution after mixing 40 µl (1 assay unit) of the HVJ-envelope vector with 4 µl of the enclosing factor. Then, 10 µl siRNA solution was added, and the mixture was kept on ice for 5 min. The final concentration of siRNA was 5 µg/10 µl. The knockdown efficacy of siRNA used in this study was examined using Lewis lung carcinoma cells, which expressed Tmem45b.

Implantation of a chronic intrathecal catheter for siRNA administration

A chronic intrathecal (i.t.) catheter was implanted into the intrathecal space, as reported previously[22]. In brief, a polyurethane i.t. catheter with an inner diameter of 0.35 mm and an outer diameter of 0.84 mm (R-ITC; Neuroscience Inc., Tokyo, Japan) was inserted 5 mm cephalad into the mouse lumbar subarachnoid space at the L4/L5 intervertebral space, with the tip of the catheter located near the lumbar enlargement of the spinal cord, under general anesthesia with 3% sevoflurane in 100% oxygen via a nose cone. The catheter was tunneled subcutaneously and externalized through the skin in the neck region. The volume of dead space of the intrathecal catheter was 3 µl. The effects of i.t. lidocaine (2%, 2 µl) were examined one day after implantation of the catheter. Animals that had shown complete paralysis of the tail and bilateral hind legs after i.t. lidocaine

were exclusively used in the following experiments. Every day, for three days after surgery, 10,000 units/kg of penicillin was injected subcutaneously to prevent infection. Following the surgeries, mice that showed paralysis or impaired motor function were excluded from this study. In 21 of the 22 mice, the catheter implantation procedure was performed successfully.

Knockdown of Tmem45b in dorsal root ganglions

Using a microinjection syringe (Hamilton) connected to an i.t. catheter under brief general anesthesia (sevoflurane in oxygen), administration of i.t. siRNA was accomplished. Over a 10-s period with a single injection volume of 5 μg /10 μl followed by a flush of physiological saline (3 μl), siRNA against *Tmem45b* or scrambled siRNA was manually administered. Mice fully recovered within 2 min after discontinuance of general anesthesia. For 3 consecutive days, injections were given daily.

Pain models

We used the following mouse model of pain:

Inflammatory pain

Mice were lightly anesthetized using inhaled 3% sevoflurane and then were injected into the plantar surface of the left hind paw, with 20 μL of complete Freund's adjuvant (CFA) (Sigma Aldrich)[23].

Skin incision-induced tissue injury pain

Using inhaled 3% sevoflurane, mice were lightly anesthetized. A plantar incision was made according to a

modification of a previous report[24]. Through skin and fascia of the plantar surface of the foot, a 5-mm longitudinal incision was made with a number 11 scalpel blade. Started 2 mm from the proximal edge of the heel, the incision was extended distally. Using curved forceps, the underlying muscle was elevated, which left the muscle origin and insertion intact. The skin was sutured with a 7-0 nylon mattress suture and then covered with antibiotic ointment after wound hemostasis.

Peripheral nerve injury-induced neuropathic pain

Surgery was performed as previously described[25]. Using inhaled 3% sevoflurane, mice were lightly anesthetized. The left hind limb was shaved using trimmers and then sterilized using betadine and ethanol. To expose the three branches of the sciatic nerve, a small incision was made on the skin of the leg proximal to the knee and the skin and underlying muscle opened by blunt dissection. Tightly ligated with 6-0 nylon sutures, the peroneal and sural branches were transected below the ligature, and a 2–3-mm section distal to the ligature was removed. The tibial nerve was carefully avoided and left intact. The muscle tissue was closed back over the nerves and then skin was sutured shut using 6-0 nylon sutures.

Behavioral Tests

Mechanical test

On a wire mesh table for 1 hr the day before and 30 min prior to testing, mice were habituated to opaque Plexiglas chambers. Using a set of calibrated Touch Test Sensory Evaluator (North Coast Medical, Morgan

Hill, CA, USA) following the Up–Down method, testing was performed[26]. For each mouse beginning with a 0.16 g filament, the 50% paw withdrawal threshold was determined. Between the walking pads for 3 s or until a response such as a sharp withdrawal, shaking, or licking of the limb was observed, each filament was applied to the plantar surface of the hind paw. Incidents of rearing or normal ambulation during filament application were not counted. In between each application until the thresholds were determined, testing was performed with a 5-min interval.

Thermal test

According to a previous study, withdrawal latency to noxious heat stimuli was measured[27]. To the test chamber for 1 hr the day before and 30 min the day of testing, animals were placed in an acrylic chamber on a glass top table and then allowed to acclimate. A radiant heat source of constant intensity, using a Plantar Analgesia Meter (IITC Life Sciences, Woodland Hills, CA, USA), was focused on the plantar surface of the hind paw and the latency to paw withdrawal measured. Upon paw withdrawal or after 20 s of exposure to prevent injury, the heat source was shut off. With a 5-min interval between tests, the test was repeated thrice and the results for each paw were averaged together.

Evaluation of Paw Edema

By a 40 μL intraplantar injection of CFA, paw edema was induced in the hind paw of the mice. By measuring the volume of hind paw using a digital plethysmometer (Ugo Basile) under general anesthesia with 3%

sevoflurane, the edema was monitored. The results are expressed in milliliters.

Generation of Tmem45b antibody

We developed antibody to mouse Tmem45b by immunizing synthetic 264-278 amino acid peptide (GenBank # NM_144936.1) conjugated with keyhole limpet hemocyanin (KLH). In the first immunization and incomplete adjuvant, Tmem45b/KLH was emulsified with Freund's complete adjuvant (DIFCO) and then injected subcutaneously into a Japanese White Rabbit. Using the Tmem45b peptide coupled to CNBr-activated Sepharose 4B (GE Healthcare, IL, USA), serum was collected and affinity-purified after the sixth injection.

Immunohistochemistry

Mice were anesthetized using inhaled 3% sevoflurane and then perfused transcardially with phosphate-buffered saline (PBS), followed by 4% paraformaldehyde (PFA) in 0.1-M PB for DRG immunohistochemistry and by 3% glyoxal working solution (7.8 mL of 40% Glyoxal, 0.75 mL of glacial acetic acid, and 91.425 mL of ddH_2O, pH 4.0) for spinal cord immunohistochemistry. The spinal cord and dorsal root ganglia were harvested during a laminectomy. Tissues were post-fixed in 4% PFA or 3% glyoxal working solution for 2–6 hr, cryoprotected in 30% sucrose in PBS overnight, and then cut with a cryostat (Leica CM3050S, Leica, Wetzlar, Germany) into 16 μm sections for DRGs and 50 μm for spinal cord; these were then placed directly onto silane coated slides (Muto) or into wells containing PBS. Slices were blocked with 10% normal donkey

serum in PBS + 0.2% triton-X (PBS-T) for 30 min at room temperature (RT) and then incubated in primary antibody diluted in PBS-T overnight at RT for fluorescent immunostaining. Then, sections were washed in PBS-T and incubated in AlexaFluor™ secondary antibodies (Jackson ImmunoResearch, West Grove, PA, USA) diluted 1:200 in PBS-T for 2 hr at RT. Then, slices were washed in PBS-T and cover-slipped with Vectashield™ (VECTOR laboratories, Burlingame, CA, USA). Photographs were taken using confocal laser scanning microscopes (ECLIPSE C1, NIKON, Tokyo, Japan) For immunofluorescence staining at the following dilutions, the following primary antibodies were used: anti-NF200 raised in mouse (1:2000; Sigma N0142), anti-CGRP raised in guinea pig (1 μg/ml; Frontier Institute CGRP-GP-Af280), anti-TRPV1 raised in guinea pig (1 μg/ml)[28], biotinylated IB4 (1:100; Sigma L3759), anti-PGP9.5 raised in mouse (1:100; Neuromics MO25010), and anti-Tmem45b raised in rabbit (0.1 μg/ml). In spinal immunohistochemistry, TRPV1 and IB4 were used to label lamina I/outer part of lamina II and the dorsal part of lamina II inner, respectively[29,30].

Retrograde labeling

Using Fast Blue (FB; 1% in PBS, Polysciences GmbH, Germany), retrograde labeling of sensory neurons innervating the hind paw skin, tibialis anterior muscle, distal colon, and bladder was performed in B6 mice. Mice were anesthetized with 3% sevoflurane, and FB (10 μl) was injected in hind paw (n = 4) and tibialis anterior muscle (n = 4). Injections were administered with a 10 μl syringe (Hamilton) and 29.5-gauge needle.

Moreover, injection to visceral organs was administered as previously described[31]. In brief, mice were anesthetized with 3% sevoflurane, and to reveal the visceral organs, a midline laparotomy was performed. FB was injected into the wall of distal colon (n = 4, 6 injections per animal, total volume 2 µl) and the wall of bladder (n = 4, one injection per animal, 10 µl). The ventral membrane was closed and the skin was sutured shut using 6-0 nylon sutures. Animals were anesthetized by inhalation of 3% sevoflurane 7–10 days after FB injection and perfused transcardially using saline (0.9% NaCl), followed by 4% PFA in 0.1-M PB. Dissection of lumbar (L4–L5) DRG, lumbar (L3–L4) DRG, thoracolumbar (T13), and lumbosacral (S1) DRG for analysis of innervation to hind paw, tibialis anterior muscle, distal colon, and bladder, respectively, was performed. Six slices were dissected from one DRG and used for immunohistochemistry.

Fluorescence *in situ* hybridization

As previously described, fluorescence *in situ* hybridization was done[32]. To detect Tmem45b mRNA, digoxigenin (DIG) labeled cRNA probes were prepared. cDNA fragments of Tmem45b (90 –926; National Center for Biotechnology Information Reference Sequence NM_144936.1) were subcloned into the Bluescript II plasmid vector and sequenced. As described previously, preparation of cRNA probes was performed[33]. The sequence of primers used for the creation of cRNA probes is listed in Supplementary Table 2. *In vitro* transcription was performed using T7 or T3 RNA polymerase using the linearized plasmid. Using DIG labeling kits (Roche Diagnostic GmbH, Mannheim, Germany), probes were synthesized. Sections were treated with

the following incubation steps: acetylation with 0.25% acetic anhydride in 0.1 M triethanolamine-HCl, pH 8.0, for 10 min, and pre-hybridization for 1 h in hybridization buffer (50% formamide, 50 mM Tris-HCl, 0.02% Ficoll, 0.02% polyvinylpyrrolidone, 0.02% bovine serum albumin, 0.6 M NaCl, 200 g/ml tRNA, 1 mM EDTA, and 10% dextran sulfate, pH 7.5). Hybridization was performed at 63.5°C for 12 h in hybridization buffer supplemented with cRNA probes at a dilution of 1:1000. At 61°C, post-hybridization washing was done successively with 5X SSC for 30 min, 4X SSC containing 50% formamide for 30 min, 2X SSC containing 50% formamide for 30 min, and 0.1X SSC for 30 min. Sections were incubated at RT in NTE buffer (0.5 M NaCl, 0.01 M Tris-HCl, and 5 mM EDTA, pH 7.5,) for 20 min, 20 mM iodoacetamide in NTE buffer for 20 min, and TNT buffer (0.1 M Tris-HCl, 0.15 M NaCl, pH 7.5) for 5 min. Sections were incubated with DIG blocking solution (TNT buffer containing 1% blocking reagent [Roche Diagnostic GmbH] and 4% normal sheep serum) for 30 min and 0.5% tryamide signal amplification (TSA) blocking reagent (Thermo Fisher, Waltham, MA, USA) in TNT buffer for 30 min for immunohistochemical detection of DIG. Using the Cy3–TSA plus amplification kit (Thermo Fisher), fluorescence detection was done. Using peroxidase-conjugated anti-digoxigenin antibody (1:1000, 1 h; Invitrogen, Carlsbad, CA, USA), the detection was performed. Finally, sections were stained with IB4 (1:100; Sigma L3759).

Quantitative analysis for immunohistochemistry

For quantitative analysis of DRG neurons, images obtained from confocal laser scanning microscopes were

imported into the ImageJ software (NIH, Bethesda, MD). A positive cell was defined as a cell with an intensity two times greater than that of the background. Tissues were counterstained for a pan neuronal marker, PGP9.5, to visualize and measure the cross-sectional area of a neuronal cell body. Only neurons with clearly visible nuclei were counted. Quantification of date may have yielded biased estimates of actual numbers of cells and neurons because a stereological approach was not used in this study. Sections that were at least 48 μm apart were counted for each DRG to prevent duplicate counting of neuronal cell bodies.

Western blot analysis

Frozen tissues were cut into small pieces and homogenized in ice-cold lysis buffer (50 mM HEPES, 1% Triton X-100, 50 mM NaCl, 50 mM sodium fluoride, 5 mM EDTA, 10 mM sodium pyrophosphate, 1 mM phenylmethanesulfonyl fluoride, 1 mM Na_3VO_4, 10 μg/mL leupeptin and 20 μg/mL aprotinin, pH 7.5,)[34]. For 15 min at 4°C, tissue homogenates were centrifuged at 15,000 g. Using the bicinchoninic acid method, the supernatant was collected and the protein concentration was determined[35]. By mixing them with an equal volume of 2 × SDS sample buffer, samples of the protein extracts were prepared. For use at a later date, the diluted samples were boiled for 3 min and stored at −80°C. Aliquots for each sample (equivalent total protein content, 40 μg) were used in each experiment. Proteins were separated using 10% sodium-dodecyl-sulfate polyacrylamide gel electrophoresis (SDS-PAGE) and then electroblotted onto nitrocellulose membranes. The electroblotted membranes were incubated in blocking buffer (containing 20 mM Tris, 150 mM NaCl, 3%

bovine serum albumin and 0.02% sodium azide, pH 7.5) overnight at 4°C and then incubated with a rabbit anti-Tmem45b antibody (0.1 μg/ml), and a rabbit antibeta-actin antibody (1:2000; Cell Signaling 4970S). After washing again, the membrane was incubated with a secondary antibody, antirabbit IgG antibody (1:2000; Cell Signaling 7074S), for detection of Tmem45b or beta-actin. Using the enhanced chemiluminescence (ECL) system (Amersham Pharmacia Biotech, Piscataway, NJ, USA), the densities of the immunoreactive Tmem45b bands and beta-actin bands were detected

Real time quantitative PCR

All tissues were freshly isolated from adult C57BL/6N mice. The total RNA samples were extracted using the RNeasy Mini Kit (Qiagen, Hilden, Germany). Using the PrimeScript RT Master Mix (Takara, Japan), the first strand cDNA was synthesized. The templates were amplified using TB Green Fast qPCR Mix (Takara, Japan). Experiments were carried out in triplicates using the LightCycler480 (Roche Diagnostic GmbH). The product calibrations and normalizations were performed using the 2-Δcycle threshold (Ct) method (Schmittgen and Livac, 2008), where ΔCt = (Ct [target gene] − Ct [reference gene]). For the analysis of mRNA expression in different tissues, Gapdh was used as a reference gene. The sequence of the primers used in quantitative PCR is listed in Supplementary Table 2.

Gene profiling

Using RNeasy Mini Kit (Qiagen, Germany) including a DNA digestion step, RNA from DRG dissected IB4-saporin or saporin injected mice (n = 3 mice per condition) was isolated. Small aliquot from each sample was subjected to a quality control test using the RNA 6000 Pico/Nano LabChip technology (Agilent Technologies, Santa Clara, CA, USA) prior to being used for a microarray. For microarray, only RNA with sharp and distinct 28 S and 18 S ribosomal RNA peaks and ratio 28 S/18 S > 1.7 or RIN > 7 was further processed[36]. According to the Affymetrix standard protocol, cRNA double T7 linear amplification was performed for each sample. A total of amplified and biotinylated cRNA was then processed on Affymetrix GeneChip™ Mouse Gene 2.0 ST Array and signal values and detection calls (present or absent) for all transcripts were assigned with GeneChip™ Command Console (TAC4.0, Affymetrix). Using the Robust Multi-array Average algorithm, Affymetrix CEL files were normalized for Bioinformatics analysis. Fold differences were calculated as the ratio between the average values within each condition. We defined a criterion of a 1.5-fold and greater difference plus fold discovery rate adjusted *p*-value of <0.1 to identify transcripts that are differentially expressed between the controls and the ablated mice.

Statistical analysis

Statistical analyses were performed in this study using JMP™ statistical software (version 14.2; SAS institute, Cary NC, USA). We have expressed quantitative data as mean ± s.d. No statistical methods were used to predetermine sample sizes, but our sample sizes were selected on the basis of previously published studies (see

Reporting Summary for references). The allocation of mice to groups was done randomly in all experiments. No animals or data points were excluded from the analyses. Prior to choosing the statistical test, normality tests and *F* tests for equality of variances were performed. For two-group comparison, statistics were based on two-sided paired or unpaired Student's *t* test or Mann-Whitney rank-sum tests. For multiple comparisons, one-way ANOVA followed by Dunnett's test or two-way ANOVA were performed, unless indicated otherwise. *P*-values <0.05 were considered as statistically significant. Statistical details of specific experiments—for instance, exact *n* values and what *n* represents, statistical tests used, and *P* values have been summarized in the figure legends.

References

21. Yamamoto, K., et al. *Mol. Pain* **14**, 1-11 (2018).

22. Furuse, S., et al. *Anesthesiology* **111**, 173-186 (2009).

23. Honore, P, et al. *Neuroscience* **98**, 585-598 (2000).

24. Banik, R.K., Woo, Y.C., Park, S.S. & Brennan, T.J. *Anesthesiology* **105,** 1246-1253 (2006).

25. Shields, S., Eckert, W.A. & Basbaum, A.I. *J. Pain* **4**, 465-470 (2003).

26. Chaplan, S.R., et al. *J. Neurosci. Methods* **53**, 55-63 (1994).

27. Barabas, M.E., & Stucky, C.L. *Mol. Pain* **9**, 9 (2013).

28. Fuseya, S., et al. *Anesthesiology* **125**, 204-218 (2016).

29. Zylka, M.J., Rice, F.L., & Anderson, D.J. *Neuron* **45**, 17–25 (2005).

30. Cavanaugh, D.J., et al. *J. Neurosci.* **31**, 10119-10127 (2011).

31. Prato, V., et al. *Cell Rep.* **11**, 3102-3115 (2017).

32. Miyazaki, T., et al. *Eur. J. Neurosci*. **33**, 82-94 (2010).

33. Yamasaki, M., et al. *J. Neurosci*. **21**, 7691-7704 (2001).

34. Molloy, C.J., Taylor, D.S. & Weber, H. *J. Biol. Chem.* **268**, 7338-7345 (1993).

35. Smith, P.K., et al. *Anal. Biochem*. **50**, 76-85 (1985).

36. Schroeder, A., et al. *BMC Molecular. Biol*. **7**, 3 (2006).

37. Choi, S., et al. *J. Physiol. Sci*. **67**, 431-438 (2017).

38. Martin, W.J., Cao, Y.Q. & Basbaum, A.I. *J Neurophysiol.* **91**, 1945-1954 (2004).

Figure 1

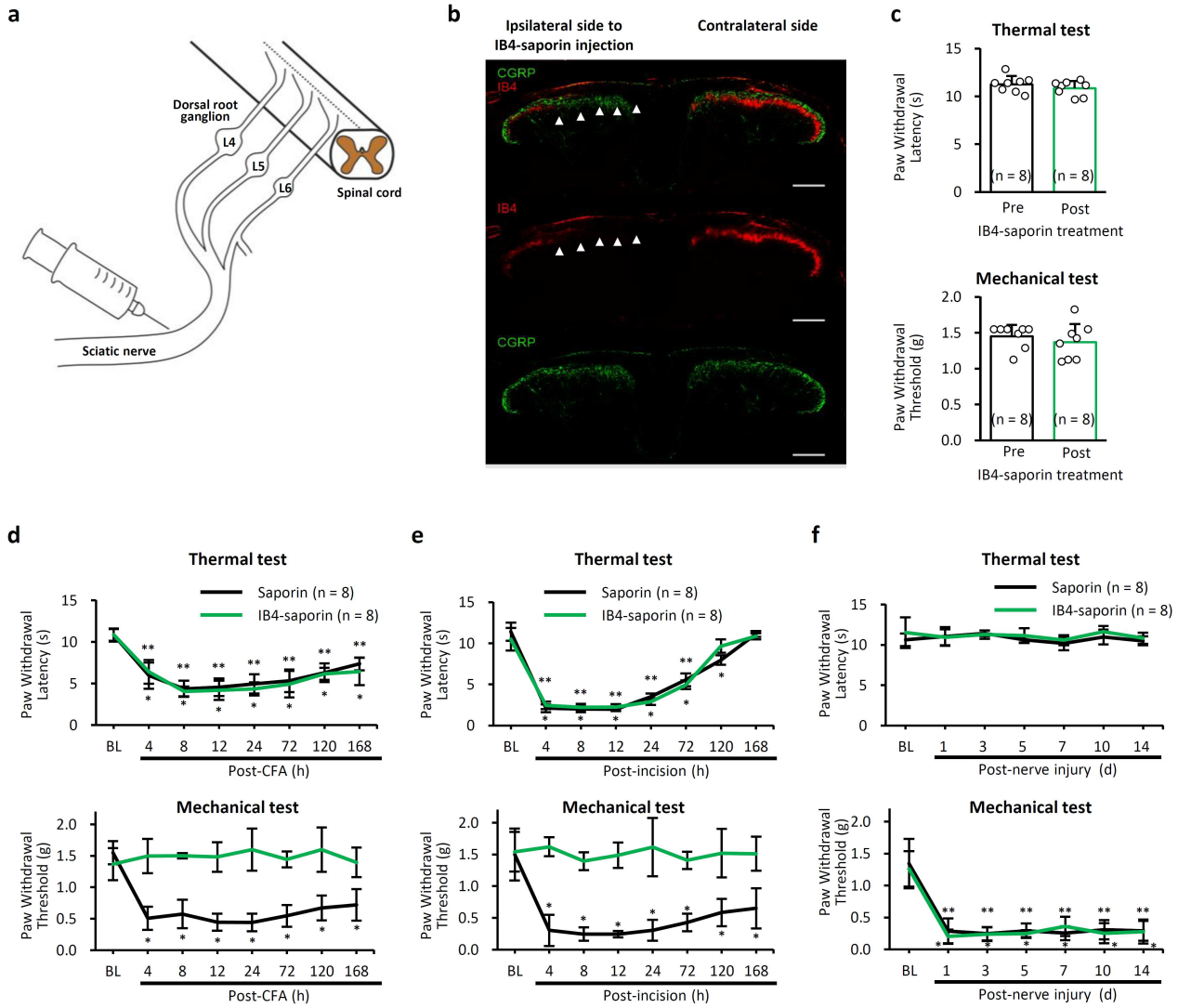
a
Dorsal root ganglion
L4
L5
L6
Spinal cord
Sciatic nerve
b
Ipsilateral side to IB4-saporin injection
Contralateral side
CGRP
IB4
IB4
CGRP
c
Thermal test
Paw Withdrawal Latency (s)
(n = 8)
(n = 8)
Pre
Post
IB4-saporin treatment
Mechanical test
Paw Withdrawal Threshold (g)
(n = 8)
(n = 8)
Pre
Post
IB4-saporin treatment
d
Thermal test
Saporin (n = 8)
IB4-saporin (n = 8)
Paw Withdrawal Latency (s)
BL 4 8 12 24 72 120 168
Post-CFA (h)
Mechanical test
Paw Withdrawal Threshold (g)
BL 4 8 12 24 72 120 168
Post-CFA (h)
e
Thermal test
Saporin (n = 8)
IB4-saporin (n = 8)
Paw Withdrawal Latency (s)
BL 4 8 12 24 72 120 168
Post-incision (h)
Mechanical test
Paw Withdrawal Threshold (g)
BL 4 8 12 24 72 120 168
Post-incision (h)
f
Thermal test
Saporin (n = 8)
IB4-saporin (n = 8)
Paw Withdrawal Latency (s)
BL 1 3 5 7 10 14
Post-nerve injury (d)
Mechanical test
Paw Withdrawal Threshold (g)
BL 1 3 5 7 10 14
Post-nerve injury (d)

Fig. 1 IB4-binding neurons are critical for inflammation and tissue injury-induced mechanical hyperalgesia. a, Schematic of IB4-saporin or saporin injection into the left sciatic nerve. **b**, IB4-saporin selectively ablated $IB4^+$ afferents (red) but not CGRP-positive afferents (green) in the dorsal horn of the spinal cord ipsilateral side to IB4-saporin injection. Immunostaining was performed 7 days after IB4-saporin injection. White arrowheads indicate elimination of $IB4^+$ afferents. Scale bar: 200 μm. **c**, Ablation of I $IB4^+$ neurons had no effect on withdrawal latencies to noxious heat stimuli nor withdrawal thresholds to von Frey filaments (before IB4-saporin injection vs 7 days after IB4-saporin injection, $P = 0.45$ for withdrawal latency, $P = 0.62$ for withdrawal threshold; two-tailed paired Student's *t*-test). **d**–**f**, Effects of IB4-saporin treatment in three different pain models (d, CFA-induced inflammation pain model; e, skin incision-induced tissue injury pain model; f, peripheral nerve injury-induced neuropathic pain model). IB4-saporin treatment selectively inhibited mechanical hyperalgesia in inflammation pain model (d) and tissue injury pain model (e). In each figure, the upper panel shows the time courses of withdrawal latency to noxious heat stimuli and the lower panel the withdrawal threshold to von Frey filaments. BL: basal value, which is a value before CFA injection, skin incision, or nerve injury. Mice receiving saporin and mice receiving IB4-saporin in each pain model, $*P < 0.0001$ vs. BL within a group comparison of mice receiving saporin, $**P < 0.0001$ vs. BL within a group comparison of mice receiving IB4-saporin; one-way ANOVA followed by Dunnett's test. All data in Fig. 1 are presented as mean ± s.d.

Figure 2

a

Fold Change	Gene Symbol	Acc number	Fold Change	Gene Symbol	Acc number
-2.24	Mrgprx1	NM_207540	-1.62	A3galt2	NM_001009819
-2.21	Mrgprb5	NM_207538	-1.60	Trpa1	NM_177781
-2.09	Mrgpra3	NM_153067	-1.59	Kcnt1	NM_175462
-2.05	Chrna6	NM_021369	-1.59	Dgki	NM_001081206
-1.93	Mrgprd	NM_203490	-1.58	Gpr165	NM_029536
-1.77	Gm16364	NR_152259	-1.57	Tmem45b	NM_144936
-1.75	Ctxn3	NM_001134697	-1.57	Kcnmb1	NM_031169
-1.75	Syt10	NM_018803	-1.57	Moxd1	NM_021509
-1.73	Rasgrp1	NM_011246	-1.56	Ano3	NM_001128103
-1.72	Hs6st2	NM_001077202	-1.55	D130009I18Rik	NR_015593
-1.71	Gm7271	NR_033501	-1.55	Gm16532	NM_001134752
-1.70	Lpar3	NM_022983	-1.54	Fam188b2-ps	NM_001142781
-1.70	Kcng3	NM_153512	-1.54	Pld5	NM_176916
-1.68	Ldb2	NM_010698	-1.54	Grik1	NM_146072
-1.66	Scn11a	NM_011887	-1.53	Paqr5	NM_028748
-1.66	Cd55	NM_010016	-1.53	Tmem255a	NM_172930
-1.65	Trpc3	NM_019510	-1.52	Prkcq	NM_008859
-1.65	Ica1l	NM_001357296	-1.52	Olfr1000	NM_001011695
-1.65	Gm21889; Gm21920		-1.51	Prkar2b	NM_011158
-1.64	Mal2	NM_178920	-1.50	Gna14	NM_008137
-1.63	Cyp4f39	NM_177307	-1.50	Slc35f4	NM_029238
-1.62	St6gal2	NM_001347403			

b

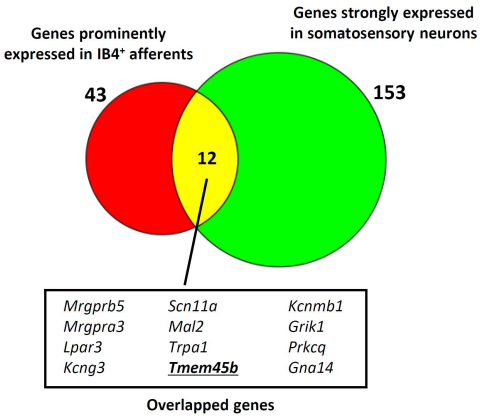

c

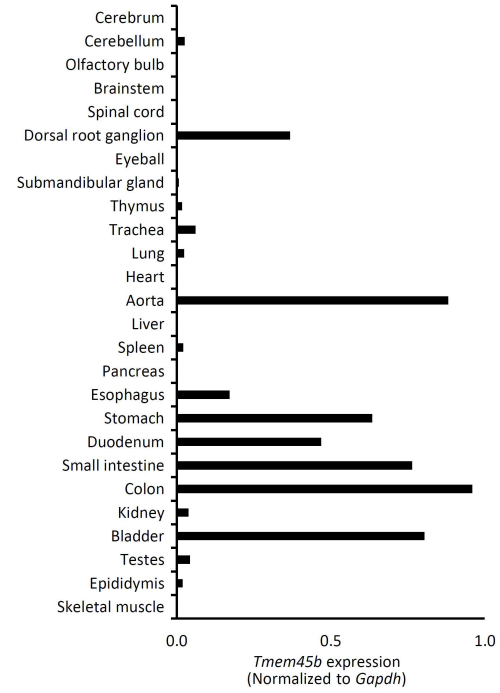

d

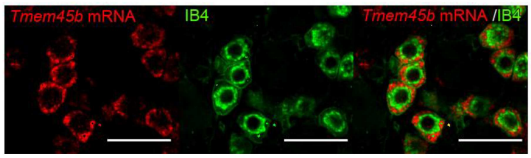

e

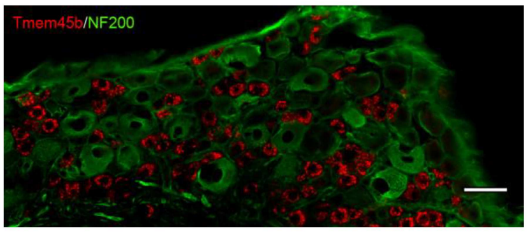

f

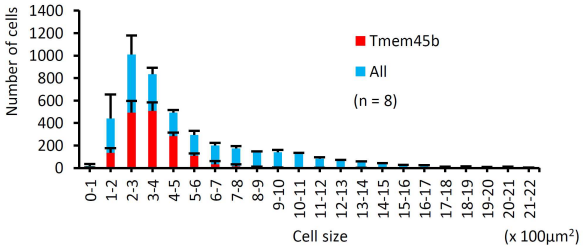

g

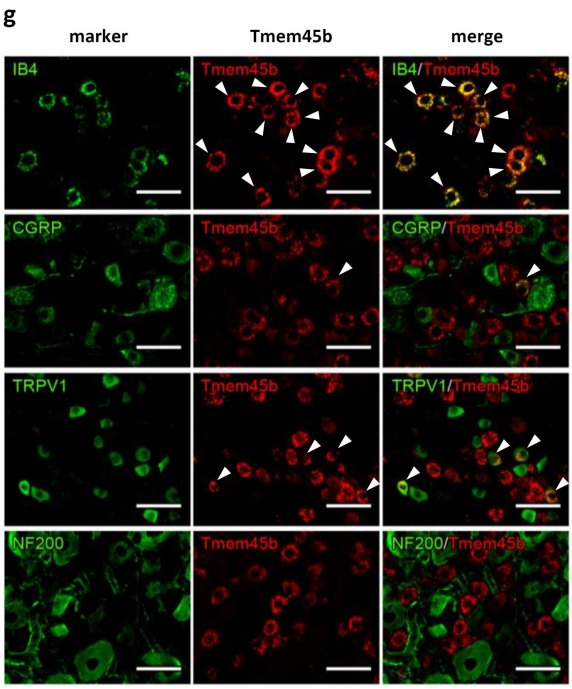

h

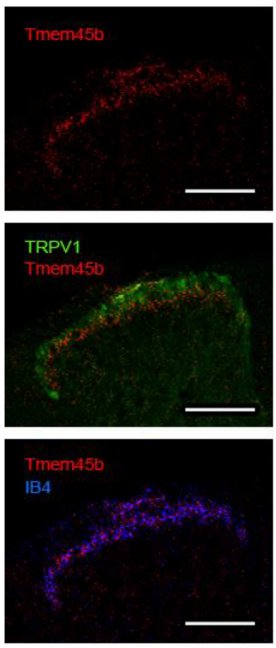

Fig. 2 Tmem45b is expressed in a specific subset of small-sized primary sensory neurons. a, Genes identified by comparison of dorsal root ganglions between mice receiving saporin and mice receiving IB4-saporin. Genes that vary >1.5-fold change (decrease) in mice receiving IB4-saproin compared with mice receiving saporin were selected to show predominent difference of expression (n = 3). **b**, Schematic of selection of interested genes. The red circle and the green circle indicate 43 genes prominently expressed in $IB4^+$ neurons and 153 genes selectively expressed in somatosensory neurons shown by Mishra et al[14], respectively. The yellow region indicates 12 overlapped genes. **c**, Real time quantitative PCR analysis revealed that *Tmem45b* was mainly expressed in DRG, aorta, bladder, and digestive tracts in mouse tissues. Bars represent *Tmem45b* mRNA expression normalized to *Gapdh*. **d**, Expression of *Tmem45b* mRNA in $IB4^+$ dorsal root ganglion (DRG) neurons. *Tmem45b* mRNA (red) and IB4 (green) were stained in DRG by fluorescent *in situ* hybridization and immunohistochemistry, respectively. Scale bar:50 μm. **e**, Representative image of Tmem45b (red) expression in DRG. NF200 (green), a marker of myelinated neurons. Scale bar:50 μm. **f**, Cell size distribution of Tmem45b in L4/5 DRGs. n = 4. **g**, Colocalization of Tmem45b (red) with neuronal markers (green) including IB4 (nonpeptidergic unmyelinated neurons), CGRP (peptidergic neurons), TRPV1 (heat and capsaicin sensitive nociceptive neurons), and NF200 in DRGs. Arrowheads indicate double positive neurons. Data of colocalization were obtained from 4 mice. A scale bar represents 50 μm. **h**, Spinal innervation of Tmem45b positive afferent. red, Tmem45b; green, TRPV1; blue, IB4. Scale bar:200 μm. All data in Fig. 2 are presented as mean ± s.d.

Figure 3

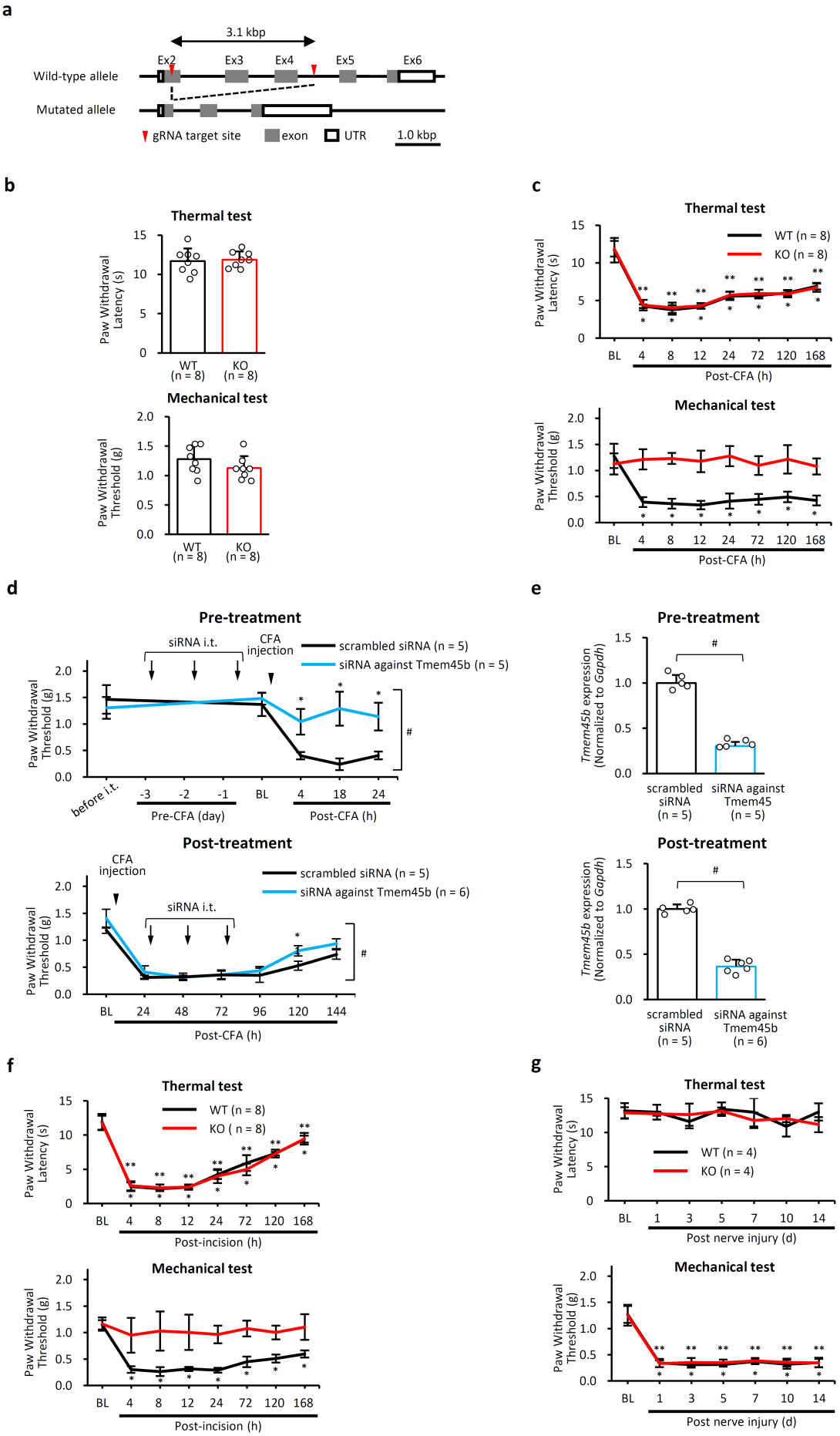
a
3.1 kbp
Ex2
Ex3
Ex4
Ex5
Ex6
Wild-type allele
Mutated allele
gRNA target site
exon
UTR
1.0 kbp
b
Thermal test
Paw Withdrawal Latency (s)
WT (n = 8)
KO (n = 8)
Mechanical test
Paw Withdrawal Threshold (g)
c
Thermal test
WT (n = 8)
KO (n = 8)
Post-CFA (h)
Mechanical test
d
Pre-treatment
siRNA i.t.
CFA injection
scrambled siRNA (n = 5)
siRNA against Tmem45b (n = 5)
before i.t.
Pre-CFA (day)
Post-CFA (h)
Post-treatment
scrambled siRNA (n = 5)
siRNA against Tmem45b (n = 6)
e
Pre-treatment
Tmem45b expression (Normalized to Gapdh)
scrambled siRNA (n = 5)
siRNA against Tmem45 (n = 5)
Post-treatment
siRNA against Tmem45b (n = 6)
f
Thermal test
WT (n = 8)
KO (n = 8)
Post-incision (h)
Mechanical test
g
Thermal test
WT (n = 4)
KO (n = 4)
Post nerve injury (d)
Mechanical test

Fig. 3 Tmem45b is critical for inflammation and tissue injury-induced mechanical hyperalgesia. a, Generation of *Tmem45b* knockout mice (KO mice). Targeting mediated by two gRNAs induced deletion of a 3.1 kbp as indicated by red arrow heads. **b**, *Tmem45b* gene knockout does not affect withdrawal latency to noxious heat stimuli (upper panel, $P = 0.91$), or withdrawal threshold to von Frey filaments (lower panel, n = 8, $P = 0.39$); two-tailed unpaired Student's *t*-test. **c**, Effects of *Tmem45b* gene knockout on hyperalgesia in CFA-induced inflammation pain model. *$P < 0.0001$ vs. BL within a group comparison of WT mice, **$P < 0.0001$ vs. BL within a group comparison of KO mice; one-way ANOVA followed by Dunnett's test. **d**, **e**, Effects of *Tmem45b* knockdown in CFA-induced inflammation pain model. **d**, Effects of pre- and post-treatment of siRNA on mechanical hyperalgesia. An upper panel and a lower panel show effects of pre- and post-treatment, respectively. SiRNA against *Tmem45b* (5 μg) or scrambled siRNA were administered 3 consecutive days before CFA injection (pre-treatment) or after CFA injection (post-treatment). Arrows indicate siRNA administration. Arrowheads indicate CFA injection. $^{\#}P < 0.0001$, siRNA against *Tmem45b* vs scramble; two-way ANOVA. *$P < 0.0002$ between group comparisons at each time point; two-tailed unpaired Student's *t*-test for analysis of pretreatment. $^{\#}P < 0.004$, siRNA vs scramble; two-way ANOVA. *$P < 0.0002$ between group comparisons at each time point; two-tailed unpaired Student's *t*-test for analysis of post-treatment. "before i.t." means a value before siRNA injection. **e**, Effects of siRNA on *Tmem45b* mRNA level in DRGs. L4/5/6 DRG samples were collected after the last behavioral assessment in both cases. A bar shows mean of relative expression level of *Tmem45b* mRNA normalized to *Gapdh*. Number of mice was the same as in Fig. 3d. $^{\#}P < 0.0001$, siRNA against *Tmem45b* vs scrambled RNA; two-tailed unpaired Student's *t*-test. **f**, **g**, Effects of *Tmem45b* gene knockout on hyperalgesia in skin incision-induced tissue injury pain model (f) and neuropathic pain model (g). *$P < 0.0001$ vs. BL within a group comparison of WT mice, **$P < 0.0001$ vs. BL within a group comparison of KO mice; one-way ANOVA followed by Dunnett's test. All data in Fig. 3 are presented as mean ± s.d. BL: basal value, corresponding to the value before CFA injection, skin incision, or nerve injury in Fig. 3.

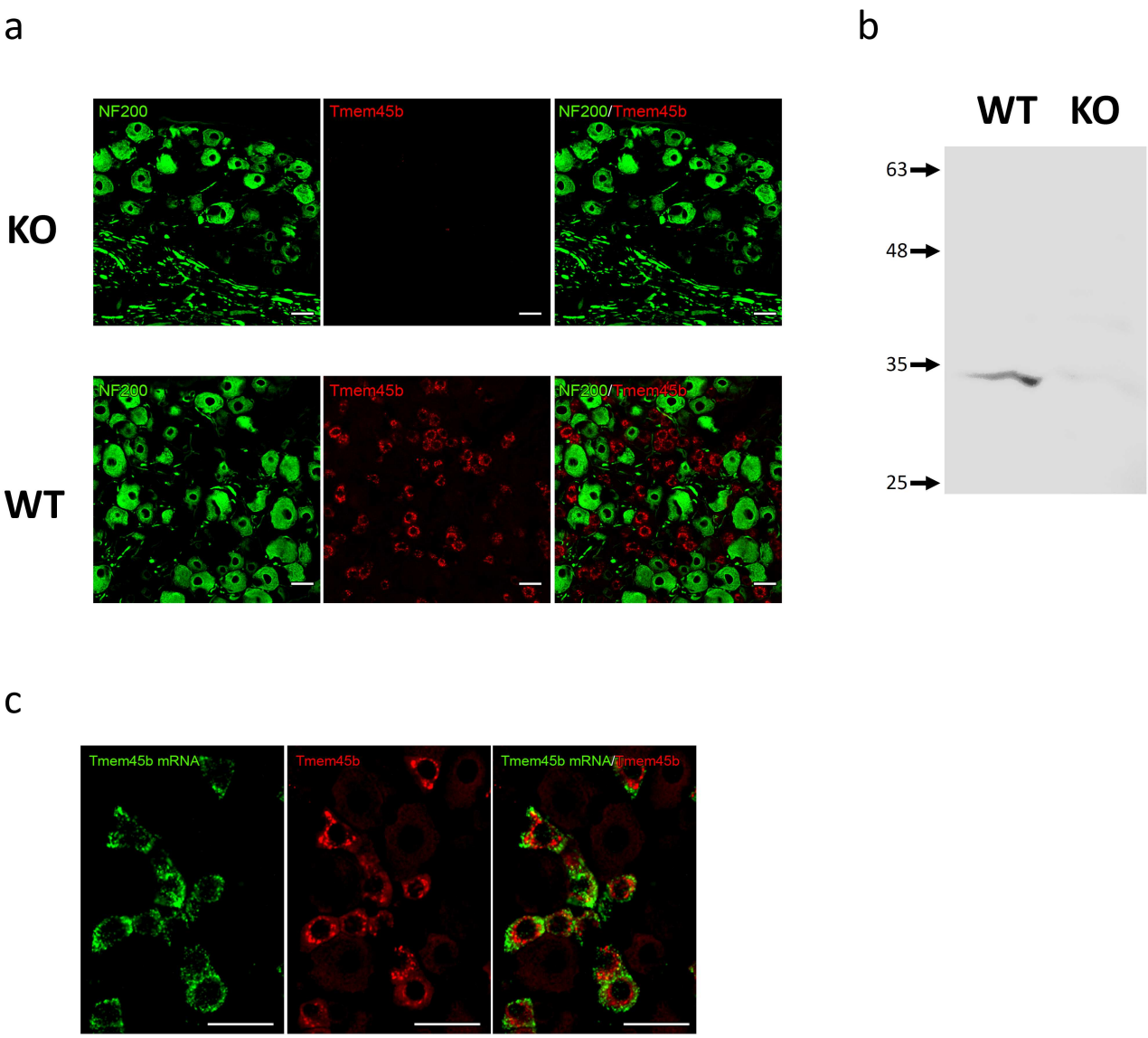

Extended Data Fig. 1 Specificity of the Tmem45b antibody. a, Immunostaining of DRG sections from WT and KO mice. A subpopulation of small-diameter DRG neurons from WT, but not *Tmem45b* KO, was recognized by our antibody. (Red, Tmem45b immunoreactivity; green, NF200 immunoreactivity). **b**, Western blot of DRG sections from WT and KO mice. Tmem45b antibody recognized a major band at around 33 kDa in the DRG of WT mice. On the other hand, no immunoreactivity was found in the DRG of KO mice. **c**, Double staining with fluorescence in situ hybridization and immunohistochemistry. The antibody selectively recognized *Tmem45b* mRNA positive neurons (Red, Tmem45b immunoreactivity; green, *Tmnem45b* mRNA). The results demonstrate that the Tmem45b antibody we generated specifically detects Tmem45b. Scale bar: 50 μm.

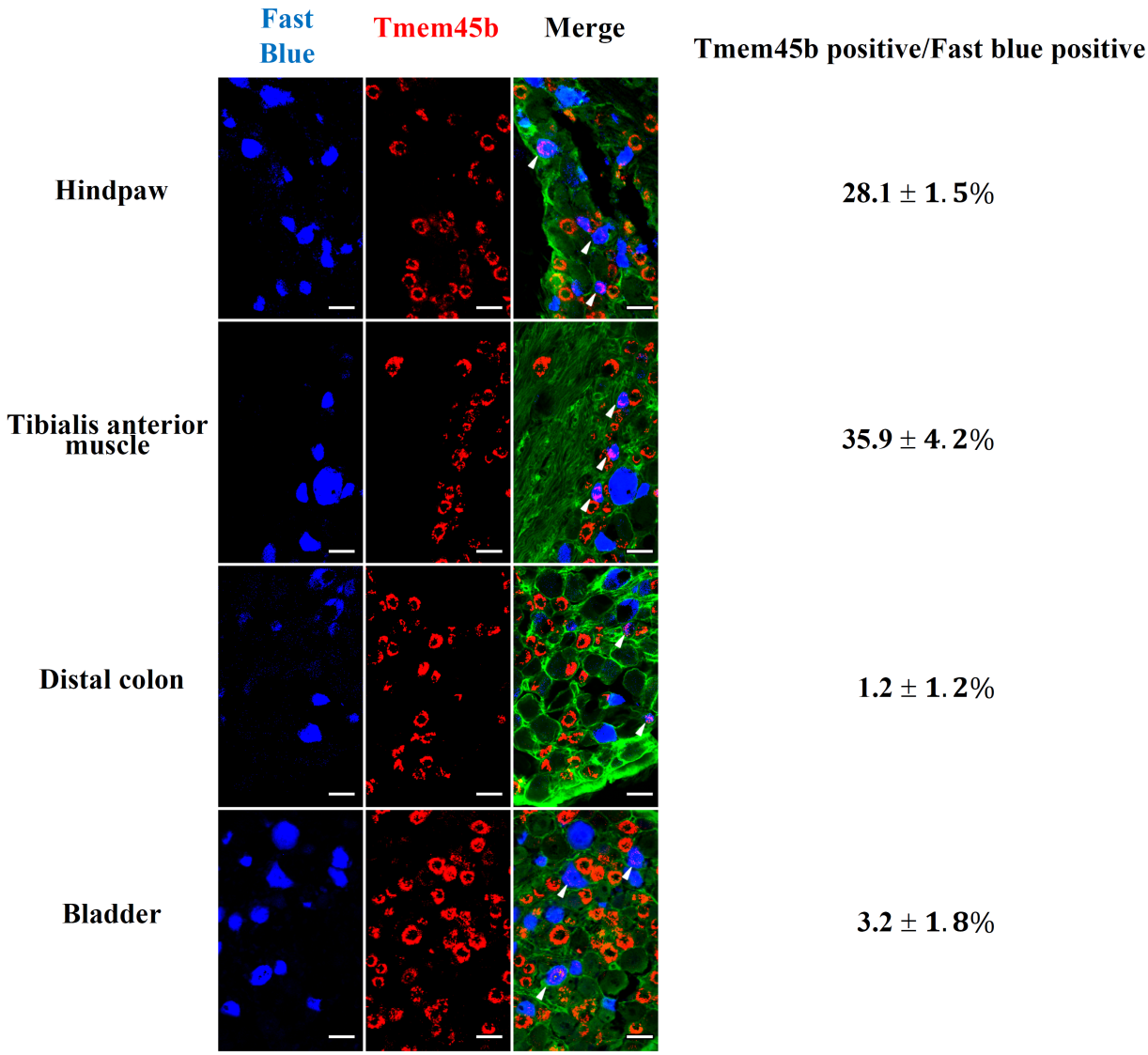

Extended Data Fig. 2 Innervation of Tmem45b positive afferents to distinct tissues. The number of Tmem45b and FB double positive neuron/FB positive neuron were 171.8 ± 27.0/612.0 ± 86.4 in hindpaw (n = 4), 128.3 ± 38.5/352.0 ± 75.3 in tibialis anterior muscle (n = 4), 5.3 ± 5.2/379.3 ± 76.3 in distal colon (n = 4), and 22.3 ± 12.1/672.0 ± 53.7 in bladder (n =4), respectively. Blue, fast blue; red, Tmem45b positive immunoreactivity; green, PGP9.5 positive immunoreactivity. White arrowheads indicate double positive neurons. Scale bar: 50 μm.

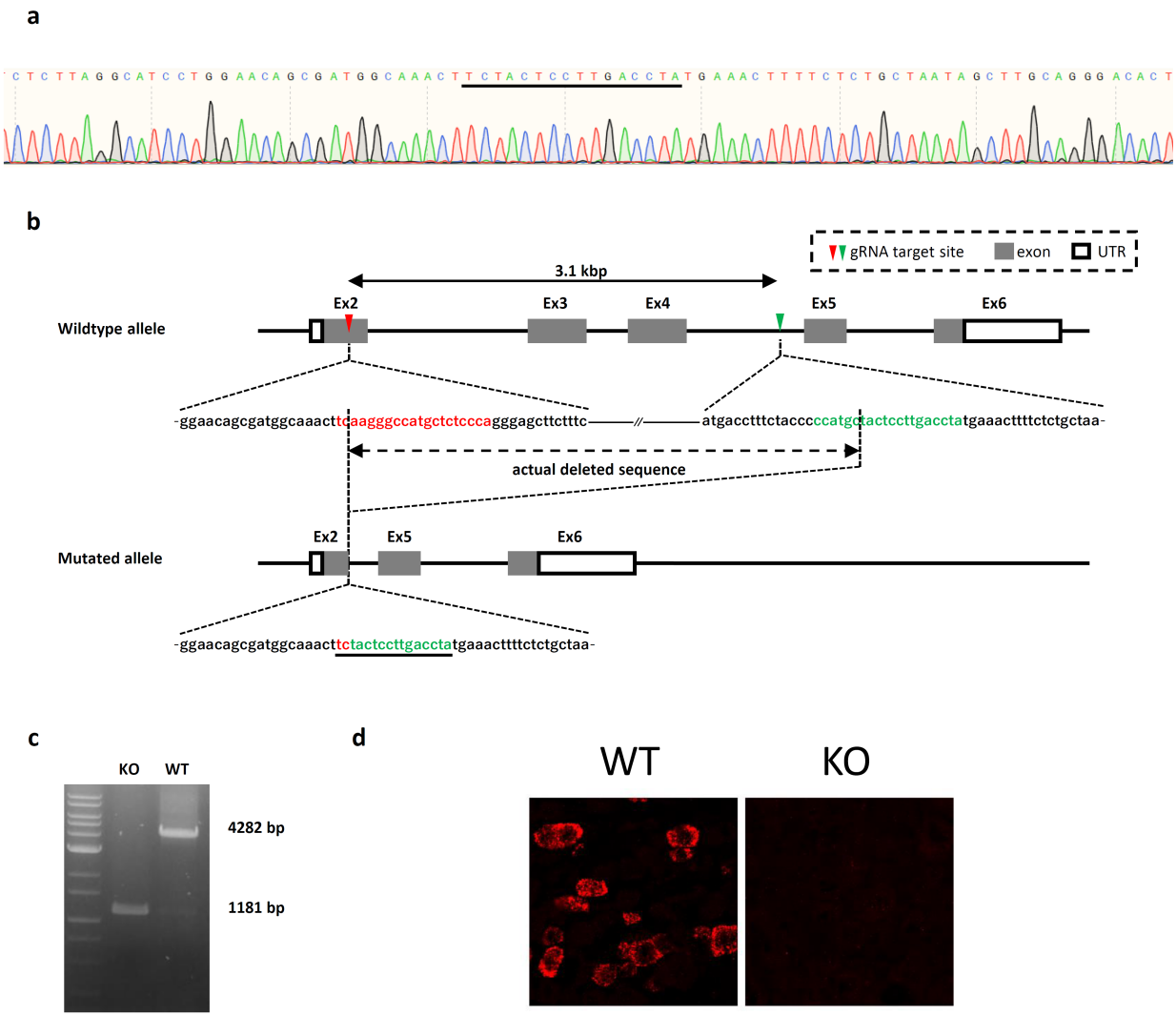

Extended Data Fig. 3 Generation of *Tmem45b* KO mice. a, Sequence chromatograms of *Tmem45b* KO mice. An underline shows the actual base sequence. **b**, Schematic illustration of deleted sequence. Exon2 contains the translational initiation codon. In an upper panel, the gRNAs were designed for the sequence labeled in red in exon 2 and for the sequence labeled in green the intron between exons 4 and 5 in wildtype allele. A dashed bi-directional arrow indicates deleted sequence determined from chromatogram. A lower panel shows mutated allele. **c**, The electrophoresis of genotyping of WT mice and *Tmem45b* KO mice using tail sample. The PCR product of *Tmem45b* KO mice is about 3.1 kbp shorter than that of WT mice as shown in supplementary figure 3a and 3b. **d**, Fluorescence in situ hybridization in DRG sections from WT and KO mice. Tmem45 mRNA was not detected in DRG of KO mice.

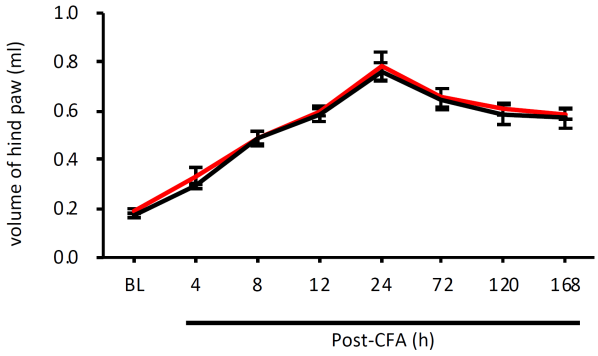

Extended Data Fig. 4 Paw edema after CFA injection. The paw volume in KO mice was comparable to that in WT mice. The time course of paw volume after CFA in KO mice injection was also comparable to that in WT mice. KO mice, n = 3 and WT mice, n = 4. BL, baseline value (value before CFA injection). *P* = 0.5885; one-way ANOVA.

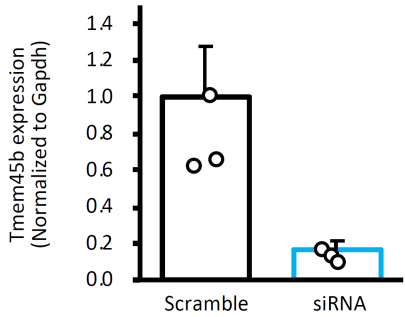

Extended Data Fig. 5 Knockdown efficacy of siRNA against *Tmem45b*. Knockdown efficacy of siRNA against *Tmem45b* used in this study was examined using Lewis lung carcinoma cells, which constitutively expressed Tmem45b. A bar shows mean of relative expression level of *Tmem45b* mRNA normalized by *Gapdh* obtained from 3 experiments. $P = 0.001$; two-tailed unpaired Student's *t* test.

Supplementary Table 1. Sequences of gRNA

Tmem45b gRNA1	TCAAGGGCCATGCTCTCCCAGTTTTAGAGCTAGAAATAGCAAGTTAAAATAAGGCTAGTCCGTTATCAACTTGAAAAAGTGGCACCGAGTCGGTGCTTTT
Tmem45b gRNA2	TAGGTCAAGGAGTAGCATGGGTTTTAGAGCTAGAAATAGCAAGTTAAAATAAGGCTAGTCCGTTATCAACTTGAAAAAGTGGCACCGAGTCGGTGCTTTT

Supplementary Table 2. Sequences of primers used in this study

Tmem45b genotyping (Tmem45b-1)	GAGAAGTCCTGTGTTAGAGTAAGGTGG
Tmem45b genotyping (Tmem45b-2)	CTAGCAGTCATCTAGACCCTGTCCTAT
Tmem45b 5'deletion sequence	TGAGGTTGTCCTCCAGCCT
Tmem45b 3'deletion sequence	ACCAGAAGCCCTATCACACA
Tmem45b cRNA probe-forward	ATGGCAAACTTCAAGGGCCATGCT
Tmem45b cRNA probe-reverse	TCACTCCTCATCCGAGCCACTCAAAAG
Tmem45b qPCR-forward	GCAATCATTGGGATCCTGGCA
Tmem45b qPCR-reverse	AGGGGCACGATGTGGAAGTA
Gapdh qPCR-forward	GGGTGTGAACCACGAGAAAT
Gapdh qPCR-reverse	ACTGTGGTCATGAGCCCTTC

Supplementary Table 3. Colocalization of Tmem45b with IB4, CGRP, TRPV1 and NF200 in DRG neurons.

Marker	Number of double positive neurons / number of each marker positive neurons
IB4	1174.5 ± 92.8 / 1256.8 ± 70.5
CGRP	96.0 ± 33.5 / 1368.5 ± 113.1
TRPV1	260.8 ± 63.0 / 1408.5 ± 486.2
NF200	2.3 ± 2.6 / 1443.0 ± 214.5

Seven to 8 slices of L4/5 DRGs per mouse were analyzed. Data from 4 mice were averaged.

Supplementary Files

This is a list of supplementary files associated with this preprint. Click to download.

- nreditorialpolicychecklist.pdf
- nrreportingsummary.pdf